Supplementary Materials for

Shifts in above- and belowground trait dissimilarity under competition mediate the future impact of neighbours

The file includes:

Supplementary Text
Tables S1 to S7
Figures S1 to S19

Supplementary Method

Appendix S1: Trait measurements

To measure leaf traits, we randomly collected up to 10 mature, healthy leaves per individual at 5:00 a.m. and transported them to the laboratory in a chilled incubator. Leaf fresh mass was measured with an electronic balance, and leaf area (LA) was quantified using an LI-3100C area meter (Li-Cor, Lincoln, Nebraska, USA). Mean leaf area was calculated as the total area divided by the leaf number. Leaf toughness was assessed on three randomly selected leaves per individual by using a digital force gauge (accuracy: 0.001 N; HADPI, Yueqing Aideburg, China) via puncture tests. We moved the gauge's 1-mm diameter probe downward at a constant speed of 10 mm/s into leaf areas that avoided primary and secondary veins. We repeated the measurement three times at different positions on each leaf and averaged the maximum penetration forces to determine leaf hardness. Force values were recorded in grams (g). All leaves were oven-dried at 75 °C to a constant mass for dry biomass (g). We calculated the leaf dry matter content as the ratio of dry biomass to fresh mass and the specific leaf area as the ratio of leaf area to dry biomass.

After measuring leaf traits, we harvested all saplings to further analyse their stems, fine-root traits, and biomass. We divided each sapling at the base into aboveground and belowground parts and collected a 5-cm segment of the main stem just above the base for stem-specific density measurement. The fresh volume of these stem segments was determined using the water displacement method. We then dried the segments in a well-ventilated oven at 75 °C for 72 hours until constant weight was reached and recorded as stem dry weight. We calculated stem-specific density as the ratio of stem dry weight to fresh volume. Additionally, we measured plant height using a measuring tape to record the distance from the stem base to the tip of the tallest leaf.

To measure fine-root traits, we thoroughly rinsed the excavated roots in a 2-mm sieve to remove all soil and organic debris. We then randomly selected approximately 2 g of fine roots (diameter < 2 mm), arranged them on a transparent tray to prevent overlap, and scanned them at 400 dpi using an Epson Expression 10000XL root scanner (Epson, Nagano, Japan). After scanning, we oven-dried the fine-root samples at 75 °C to constant mass for dry weight determination. Prior to analysis, we removed background artefacts such as shadows and stains from all images using Adobe Photoshop to ensure data accuracy. The processed images were then analysed with WinRHIZO (Arabidopsis version 2012b, Regents Instruments Inc., Quebec, Canada) to quantify total root length (cm), surface area (cm^2), volume (cm^3), and mean root diameter (mm). We calculated specific root length (cm/g) as the ratio of total root length to fine-root dry biomass and root tissue density (g/cm^3) as the ratio of fine-root dry weight (g) to volume (cm^3).

Finally, we oven-dried all remaining above- and belowground tissues (excluding those sampled for trait measurements) at 75 °C for 72 hours to determine total biomass. We calculated total aboveground biomass as the sum of the dry weights of leaves, stems, and other aboveground parts and total root biomass as the combined dry weights of fine roots and other root fractions.

Tables

Table S1 | Functional traits measured in this study and expected trait-specific responses of interspecific trait dissimilarity (ITD) to competition.

Trait	Expected ITD response	Mechanistic interpretation with direction-specific evidence.
Plant height	ITD ↓	Height mediates strongly asymmetric light competition. Empirical studies have shown that neighbor interactions suppress shorter individuals or induce compensatory elongation, reducing interspecific height differences and leading to ITD convergence (Carmona et al., 2019; Kunstler et al., 2016; Lyu et al., 2017; Mahaut et al., 2023; Yin et al., 2021).
Leaf area (LA)	ITD ↓	Large leaves enhance shading and amplify competitive effects, favoring a narrow range of effective canopy sizes under strong light competition, resulting in LA convergence (Bennett et al., 2016; Kraft et al., 2014; Lyu & Alexander, 2024; Mahaut et al., 2023).
	ITD ↑	In more heterogeneous or multispecies contexts, divergence in leaf area reduces spatial overlap in light interception and weakens neighbor effects, maintaining or increasing ITD (Lyu & Alexander, 2024; Wagg et al., 2017).
Specific leaf area (SLA)	ITD ↓	SLA reflects differences in growth rate and light capture efficiency. Competitive environments tend to filter toward SLA values associated with effective growth, producing convergence in SLA-based ITD (Bennett et al., 2016; Carmona et al., 2019; Kunstler et al., 2012; Wagg et al., 2017).
Leaf dry matter content (LDMC)	ITD ↓	Under strong competition, LDMC differences can be reduced as neighbor interactions that favor similar leaf construction strategies associated with persistence, leading to convergence (Kraft et al., 2015; Lyu & Alexander, 2024).
	ITD ↑	When expressed jointly with other leaf and belowground traits, LDMC differences can be maintained as alternative resource-use strategies, resulting in the divergence of LDMC-based ITD (Pérez-Ramos et al., 2019).
Leaf toughness (LTO)	ITD ↓	Leaf toughness enhances tolerance to chronic suppression. Competitive filtering can therefore favor mechanically robust leaves, reducing interspecific differences and leading to ITD convergence (Yang et al., 2024).
Specific stem density (SSD)	ITD ↓	SSD reflects a growth–persistence trade-off. Neighbor competition tends to filter species toward similar stem construction strategies associated with effective height gain or mechanical resistance, reducing SSD-based ITD (Kunstler et al., 2012, 2016; Yin et al., 2021).
Specific root length (SRL)	ITD ↑	SRL captures fine-root foraging efficiency. Greater SRL dissimilarity reduces overlap in soil resource exploitation, weakening belowground competition and promoting divergence in SRL-based ITD (Bennett et al., 2016; Fort et al., 2014; Lyu & Alexander, 2024).

Root diameter (RD)	ITD↓	Competitive stress can induce plastic root thickening across species, reducing interspecific differences in root diameter and leading to convergence (Bennett et al., 2016; Pérez-Ramos et al., 2019).
Root tissue density (RTD)	ITD↓	Intense belowground competition acts as a filter, favoring acquisitive root strategies (i.e., lower RTD) that enhance rapid soil resource uptake. This competitive sorting reduces interspecific variation in root construction toward a narrow range of efficient foraging phenotypes, leading to convergence in RTD-based ITD (Lyu & Alexander, 2024).

Table S2 | Tree species initially selected for our experiment and their growth forms. Species names in bold indicate those ultimately included in this study; others were excluded because of low germination rates.

Latin name	Abbr. †	Genus	Family	Growth form	Number of seedlings	Height of transplanted seedlings (cm)
Quercus chenii	QC	Quercus	Fagaceae	DC‡	1600	18.0–25.1
Hovenia acerba	HA	Hovenia	Rhamnaceae	DC	1300	12.5–17.2
Castanopsis sclerophylla	CS	Castanopsis	Fagaceae	EG	1100	6.2–9.8
Schima superba	SS	Schima	Theaceae	EG	1100	6.1–8.3
Cyclobalanopsis glauca	CG	Cyclobalanopsis	Fagaceae	EG	1400	8.1–12.3
Daphniphyllum oldhami	DO	Daphniphyllum	Daphniphyllaceae	EG	1100	7.0–9.7
Lithocarpus glaber	LG	Lithocarpus	Fagaceae	EG	1300	7.1–10.0
Phoebe chekiangensis	PC	Phoebe	Lauraceae	EG	500	7.6–9.0
Aphananthe aspera	AA	Aphananthe	Ulmaceae	DC	200	13.5–18.9
Celtis sinensis	CS	Celtis	Ulmaceae	DC	200	16.1–23.4
Mallotus japonicus	MJ	Mallotus	Euphorbiaceae	DC	400	15.3–21.0
Elaeocarpus decipiens	ED	Elaeocarpus	Elaeocarpaceae	EG	500	9.1–14.5
Ilex micrococca	IM	Ilex	Aquifoliaceae	EG	500	6.3–8.5

†: Abbreviation of species name; ‡: DC: deciduous species; EG: evergreen species

Table S3 | Light intensity, soil moisture, and soil phosphorus (total and effective) measurements across nine environmental blocks.

Environment block	Light (μmol/(m²·s))	Soil Moisture (%)	Soil phosphorus TP (g/kg)	AP (mg/kg)
Block 1	High 1237.20 ± 195.45	High 33.00±0.36	Low 0.66±0.07	Low 139.03±34.81
Block 2	High 1237.20 ± 195.45	Low 17.91±0.25	High 1.1±0.06	High 364.55±10.89
Block 3	High 1237.20 ± 195.45	Medium 29.91±0.24	Medium 0.92±0.02	Medium 154.12±6.23
Block 4	Low 14.54 ± 1.99	Medium 27.83±0.16	Low 0.33±0.00	Low 2.98±0.33
Block 5	Low 14.54 ± 1.99	Low 26.81±0.39	Medium 0.95±0.02	Medium 255.13±13.75
Block 6	Low 14.54 ± 1.99	High 31.92±0.31	High 0.98±0.04	High 267.03±12.23
Block 7	Medium 502.91 ± 103.09	High 34.20±0.16	Medium 0.80±0.01	Medium 172.42±6.07
Block 8	Medium 502.91 ± 103.09	Low 19.35±0.21	Low 0.49±0.01	Low 24.11±1.97
Block 9	Medium 502.91 ± 103.09	Medium 28.55±0.27	High 1.15±0.04	High 253.08±20.60

Note: TP: total phosphorus; AP: available phosphorus; light intensity was quantified as the maximum value and standard error of the light intensity during a summer day from 8:00 AM to 5:00 PM.

Table S4 | Effective annual sample sizes and their proportions relative to the total sample size used to construct multidimensional trait spaces (aboveground, belowground, and total) and unidimensional traits. Leaf area, specific leaf area, leaf dry matter content, leaf toughness, and stem-specific density were used for the aboveground trait space; specific root length, root diameter, and root tissue density were used for the belowground space; and all traits were used for the total space.

Trait	Number of seedlings (% completeness)		
	1st year	2nd year	3rd year
aboveground trait space	615(97.62%)	1941(81.18%)	1453(51.95%)
belowground trait space	625 (99.21%)	2272 (95.02%)	1608 (57.49%)
total trait space	613 (97.3%)	1938 (81.05%)	1380 (49.34%)
leaf area (LA, cm^2)	622 (98.73%)	1971 (82.43%)	1482 (52.99%)
specific leaf area (SLA, cm^2/g)	622 (98.73%)	1971 (82.43%)	1476 (52.77%)
leaf dry matter content (LDMC, g/g)	622 (98.73%)	1971 (82.43%)	1484 (53.06%)
leaf toughness (LTO, GN)	618 (98.1%)	1972 (82.48%)	1484 (53.06%)
specific stem density (SSD, g/cm^3)	626 (99.37%)	2276 (95.19%)	1816 (64.93%)
plant height (Height, cm)	630 (100%)	2295 (95.98%)	2164 (77.37%)
specific root length (SRL, m/g)	625 (99.21%)	2272 (95.02%)	1608 (57.49%)
root diameter (RD, mm)	626 (99.37%)	2273 (95.06%)	1627 (58.17%)
root tissue density (RTD, g/cm^3)	625 (99.21%)	2272 (95.02%)	1608 (57.49%)
total sample size	630 seedings	2391 seedlings	2797 seedlings

Table S5 | Principal component analysis (PCA) results showing trait loadings and variance explained for aboveground traits, fine root traits, and combined traits. The first three principal components were retained for the aboveground trait space (66.91% of the variance explained), the first two components were retained for the fine root trait space (94.87% of the variance explained), and the first four components were retained for the combined trait set. Component selection was guided by Horn's parallel analysis.

Organ	Trait	PC1	PC2	PC3	PC4	PC5	PC6	PC7	PC8	PC9
Above-ground (n=4009)	LA	0.31	0.14	**0.82**	0.33	0.33	0.04	—	—	—
	SLA	**0.55**	0.2	-0.3	0.23	-0.19	0.69	—	—	—
	LDMC	**-0.53**	0.28	-0.12	-0.02	0.63	0.47	—	—	—
	LTO	**-0.44**	-0.4	**0.4**	0.03	-0.49	0.5	—	—	—
	SSD	-0.35	**0.52**	-0.07	0.65	-0.36	-0.22	—	—	—
	Height	0	**0.65**	0.26	-0.64	-0.3	0.05	—	—	—
	Variation (%)	39.51	27.4	16.18	7.91	6.25	2.75	—	—	—
Fine-root (n=4505)	SRL	**0.6**	0.53	0.59	—	—	—	—	—	—
	RD	**-0.73**	0.08	0.67	—	—	—	—	—	—
	RTD	0.31	**-0.84**	0.44	—	—	—	—	—	—
	Variation (%)	57	37.87	5.13	—	—	—	—	—	—
Total (n=3931)	LA	0.14	0.39	0.3	0.02	0.8	0.15	0.26	0.03	0.02
	SLA	**0.42**	0.35	-0.32	0.16	-0.16	0.22	-0.15	0.68	0.15
	LDMC	**-0.48**	-0.17	-0.28	-0.24	0.08	-0.09	0.6	0.47	0.1
	LTO	-0.3	-0.36	**0.49**	0.07	0.18	0.04	-0.51	0.49	0.07
	SSD	**-0.43**	0.11	-0.4	-0.12	0.16	0.68	-0.31	-0.21	0.03
	Height	-0.21	**0.46**	-0.22	-0.32	0.16	-0.63	-0.42	0.02	-0.01
	SRL	0.35	-0.23	0.06	**-0.68**	0.04	0.08	-0.06	-0.08	0.59
	RD	-0.34	**0.41**	0.3	0.27	-0.31	0	0.11	-0.11	0.65
	RTD	0.07	-0.35	**-0.43**	**0.51**	0.38	-0.25	-0.09	-0.13	0.43
	Variation (%)	28.35	23.91	15.24	12.65	7.9	4.76	3.92	1.79	1.48

Table S6 | Summary of the model evaluating the effects of interspecific trait dissimilarity (ITD) and ITD changes on seedling competition intensity in the corresponding year. The model includes ITD and its changes in the first, second, and third years to predict seedling (N = 3185) competition intensity for the same year (e.g., ITD and ITD changes in the first year predict seedling competition in the first year). Fixed effects include ITD, ITD changes, and year, whereas species and environmental blocks are treated as random effects.

	Predictors	Estimates	CI	P value	Marginal R^2	Conditional R^2
Aboveground	Intercept	1.32	0.95 — 1.69	< 0.001	0.132	0.297
	Changes in ITD	0.29	0.14 — 0.44	< 0.001		
	ITD	-0.23	-0.35 — -0.11	< 0.001		
	year	0.07	0.05 — 0.08	< 0.001		
Belowground fine-root	Intercept	0.43	0.14 — 0.70	0.003	0.015	0.237
	Changes in ITD	0.03	-0.04 — 0.10	0.343		
	ITD	0.09	-0.04 — 0.22	0.165		
	year	0.06	0.03 — 0.09	< 0.001		

Table S7 | Summary of the model used to evaluate the effects of interspecific trait dissimilarity (ITD) and ITD changes on seedling competition intensity in the following year. The model incorporates the ITD and its changes within the first and second years to predict seedling competition intensity in the subsequent years (i.e., the second and third years; $N = 2870$). Fixed effects include ITD, ITD changes, and year, whereas species and environmental blocks are included as random effects.

	Predictors	Estimates	CI	*P* value	Marginal R^2	Conditional R^2
Aboveground	Intercept	0.91	0.57 — 1.24	< 0.001	0.038	0.204
	Changes in ITD	0.24	-0.03 — 0.52	0.085		
	ITD	-0.09	-0.21 — 0.03	0.131		
	year	0.05	0.02 — 0.09	0.003		
Belowground fine-root	Intercept	0.92	0.69 — 1.15	0.003	0.018	0.243
	Changes in ITD	-0.23	-0.31 — -0.15	< 0.001		
	ITD	-0.12	-0.21 — -0.03	0.010		
	year	0.05	0.03 — 0.08	< 0.001		

Figures

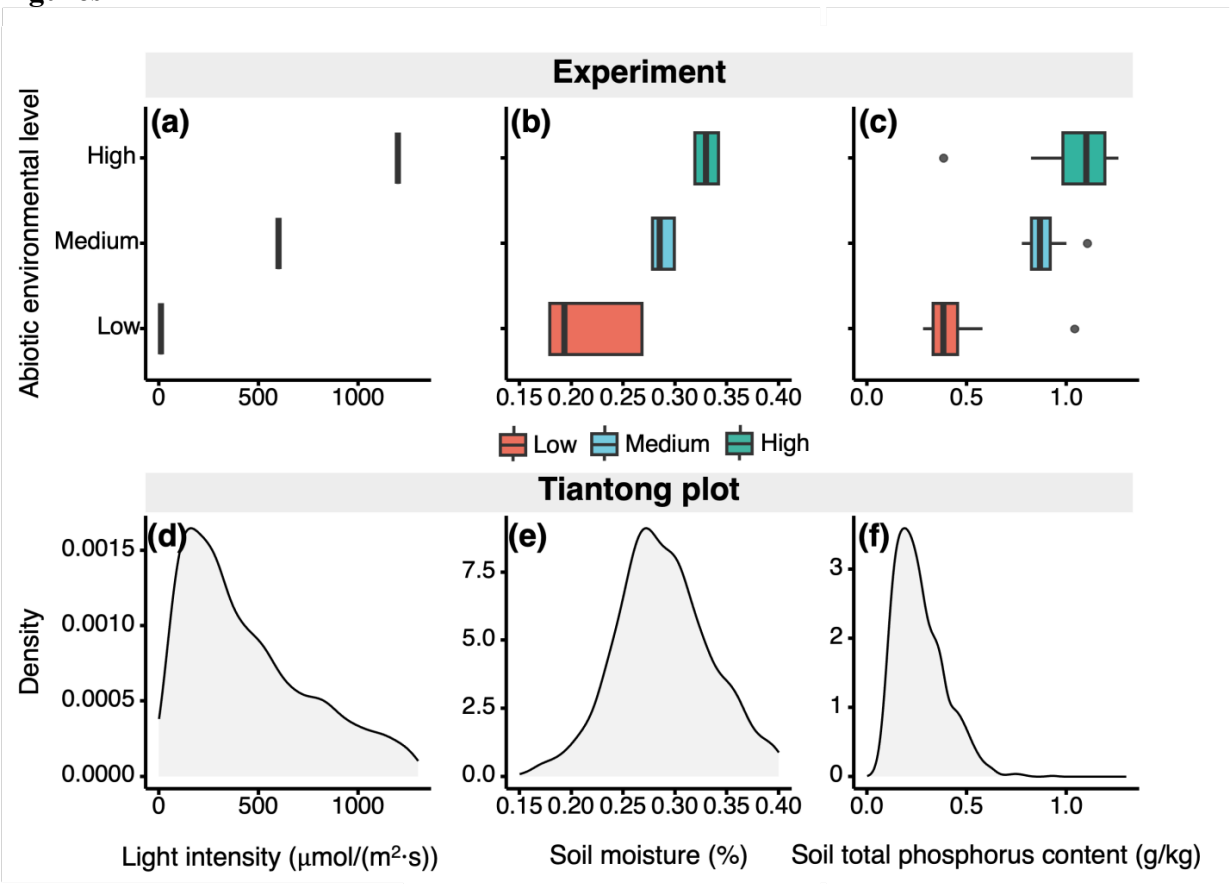

Figure S1 | Comparison of abiotic environmental conditions between the greenhouse experiment and the natural Tiantong Forest. (a–c) The three discrete levels (low, medium, and high) of light availability, soil moisture, and total soil phosphorus were manipulated in our greenhouse experiment. Detailed measurement protocols are provided in Appendix S1. (d–f) The corresponding continuous environmental gradients were measured in situ across the Tiantong plot. Corresponding continuous gradients of light, soil moisture, and total soil phosphorus across the 20-ha Tiantong Forest Dynamics Plot. Understory light availability was quantified using the LESS (Leaf-Environment Spatial Structure) model (Qi et al., 2019), which integrates LiDAR-derived canopy structure, topography, and spatial heterogeneity to estimate incident light at the forest floor (Yu et al., 2022). Soil moisture and phosphorus were sampled at 20-m intervals following standardized methods (He et al., 2022).

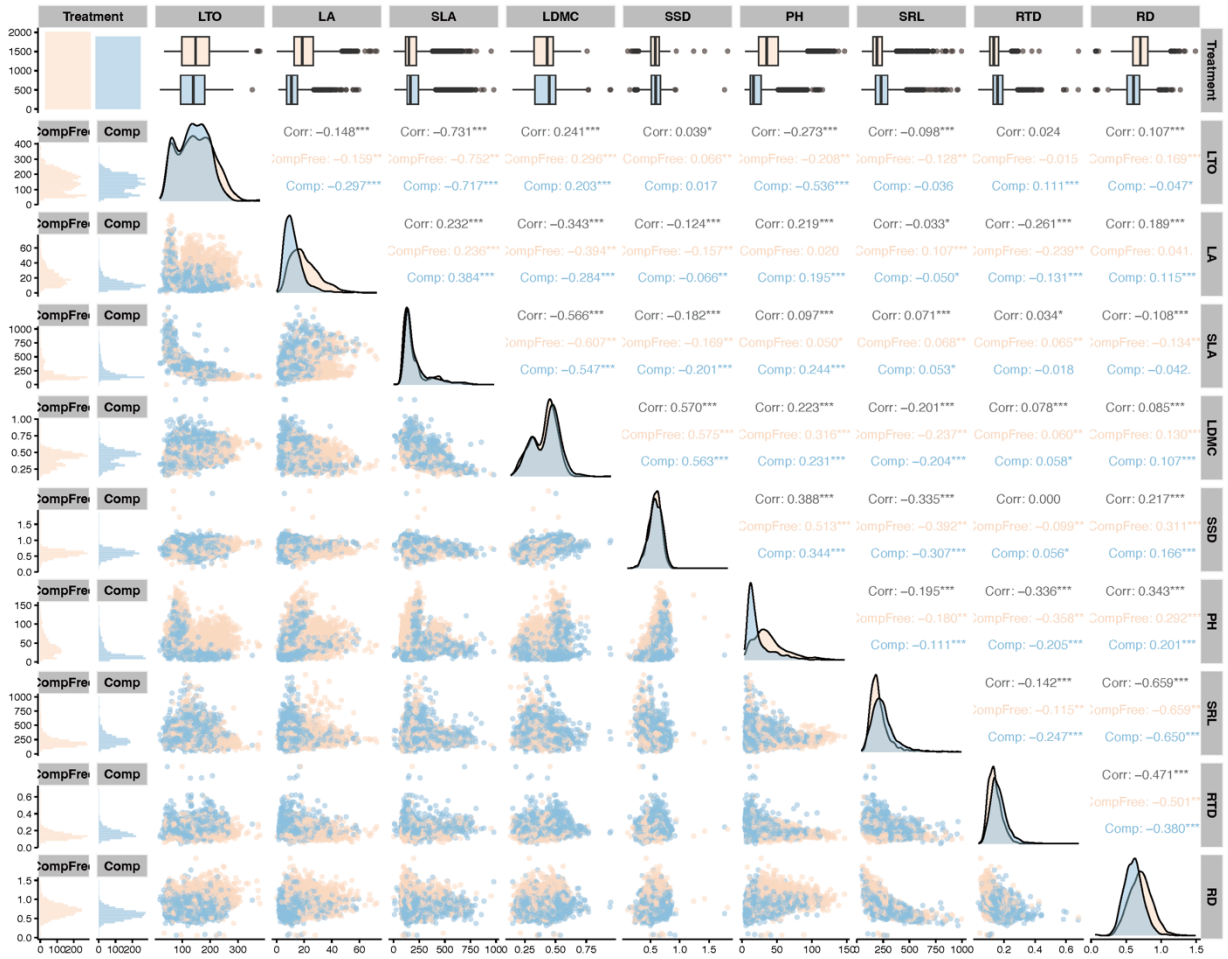

Figure S2 | Pearson correlation matrix of six aboveground traits and three fine-root traits for all the seedlings across the three experimental years. The orange points represent seedlings under the competition-free condition, whereas the blue points represent seedlings under the competition condition. The leftmost and topmost columns of the matrix display trait distributions and histograms for seedlings under the competition-free and competition conditions, respectively. The lower-left triangle of the matrix contains scatter plots showing the relationships between each pair of traits. The diagonal includes probability density functions for each trait under both conditions. The upper-right triangle presents correlation coefficient values for each trait pair. Trait abbreviations: LA (leaf area), SLA (specific leaf area), LDMC (leaf dry matter content), LT (leaf toughness), Height (shoot height), SSD (specific stem density), SRL (specific root length), RD (root diameter), and RTD (root tissue density).

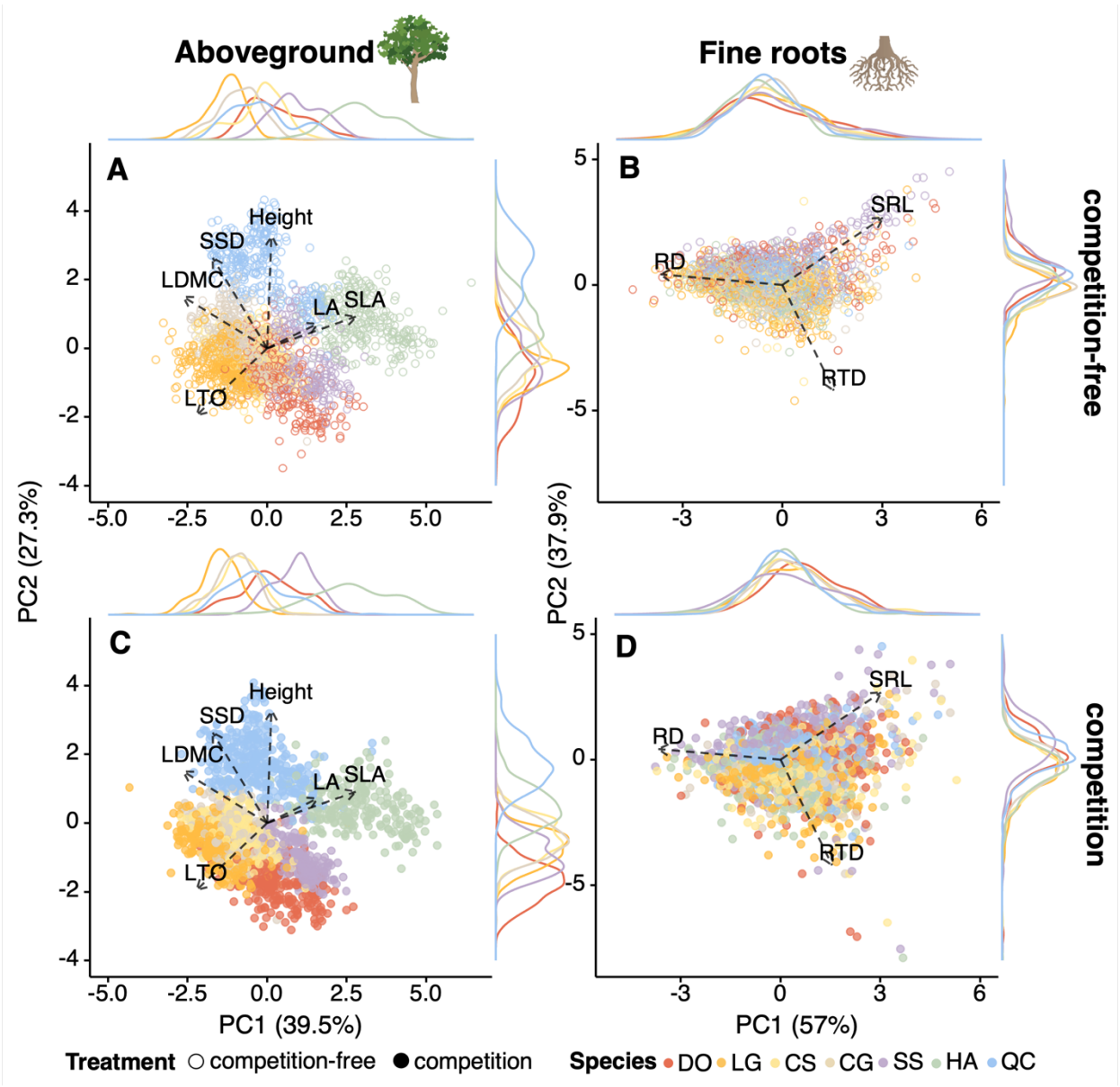

Figure S3 | Principal component analysis of seedling functional traits under different competitive conditions. PCA of six aboveground (A, C) and three belowground (B, D) traits from seedlings with complete datasets under competition-free (A, B; hollow points) and competition (C, D; solid points) conditions. Different colors represent different species. The density distribution curves show the trait distributions along the first two principal components. Table 3 shows the trait loadings and variance explained by each component.

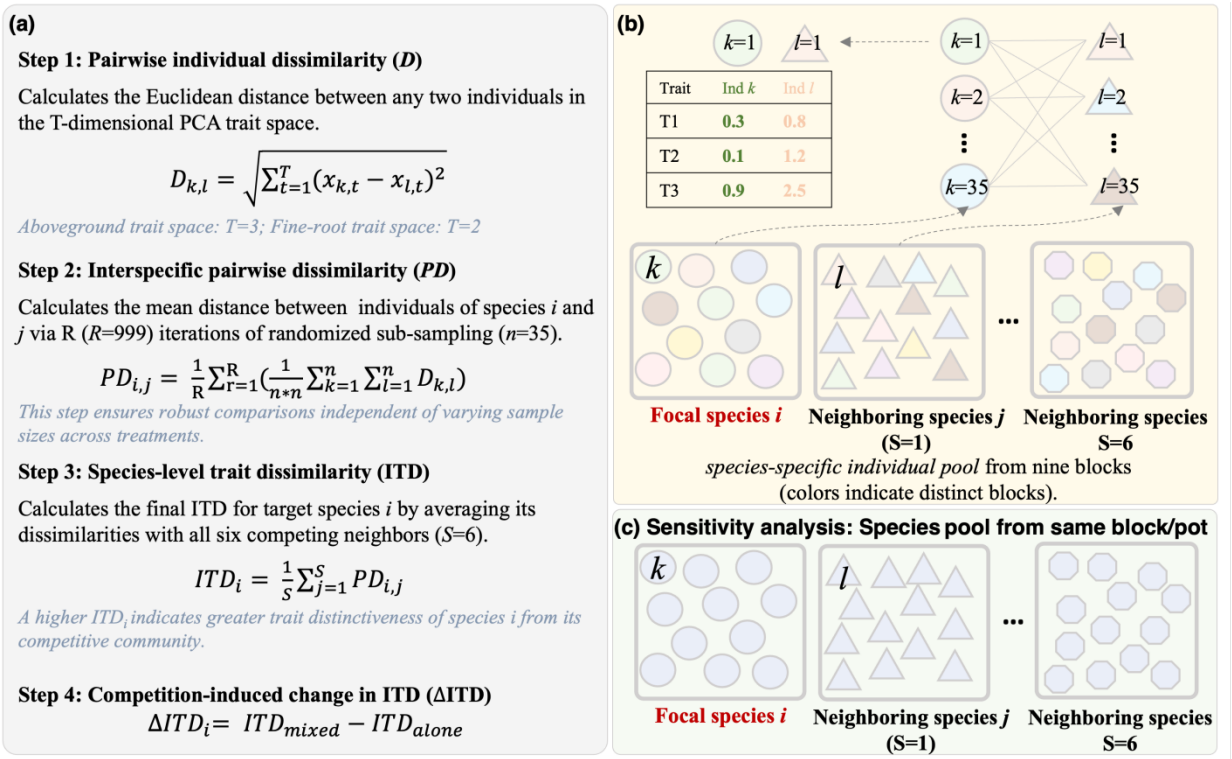

Figure S4 | Workflow for quantifying interspecific trait dissimilarity (ITD). (a) Hierarchical, individual-based calculation of ITD. Pairwise Euclidean distances were first calculated between individuals in a PCA-derived trait space. Interspecific pairwise dissimilarity between a focal species i and a neighboring species j was then estimated using repeated randomized subsampling (999 iterations; n = 35 individuals per species) to standardize the sample size. Species-level ITD was obtained by averaging pairwise dissimilarities between the focal species and its six heterospecific neighbors. Neighbor-induced change in ITD was calculated $\Delta ITD = ITD_{mixed} - ITD_{alone}$. (b) ITD estimation under spatially heterogeneous environments. Species-specific individual pools were constructed by pooling all individuals of each species across the nine environmental blocks, representing the full range of abiotic conditions in the experiment. Pairwise dissimilarities were calculated by random sampling from these pools (colors indicate blocks; shapes indicate species). (c) Sensitivity analyses under environmentally homogeneous conditions. ITD was recalculated using individuals drawn from the same pot or within-pot species assemblages in the competition treatment. Consistent results across heterogeneous (block-level) and homogeneous (pot-level) analyses indicate that ITD patterns are robust to environmental heterogeneity.

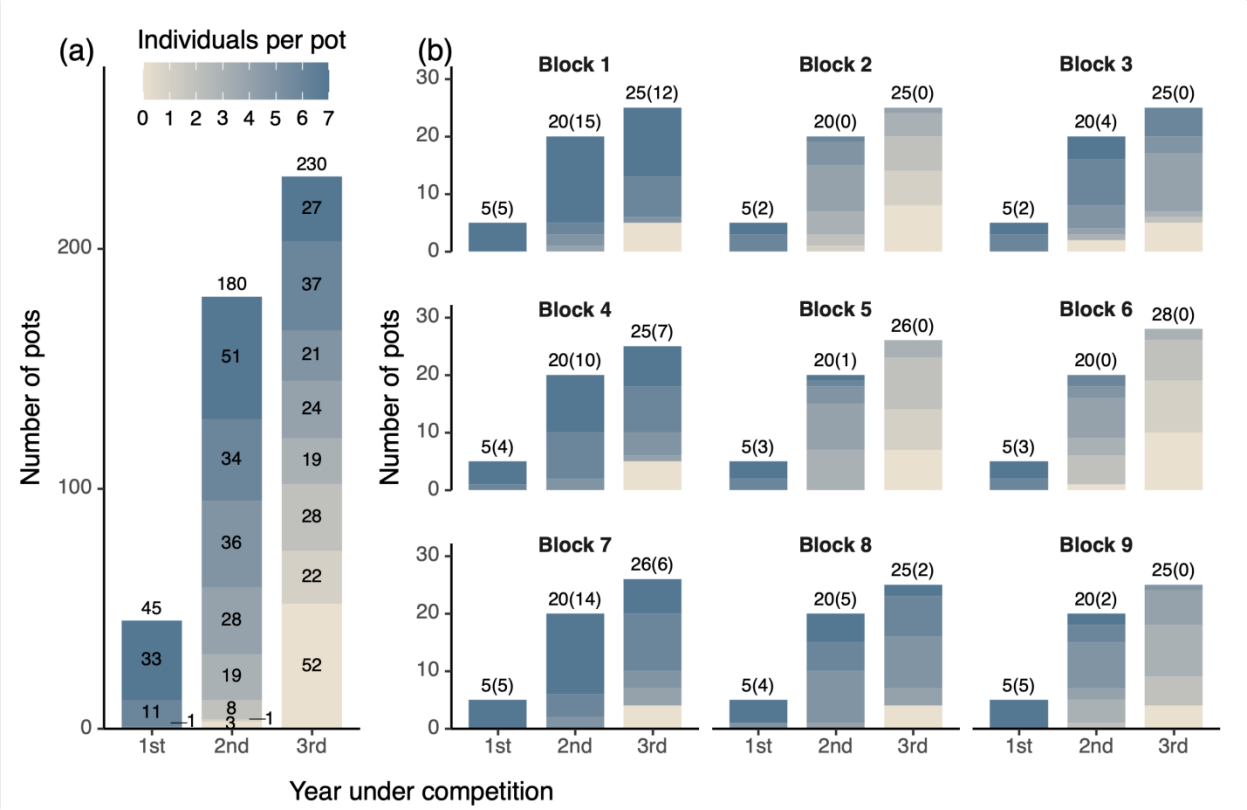

Figure S5 | Availability of seedlings for constructing the aboveground trait space under competition. (a) Distribution of the number of individuals per pot with complete aboveground trait data across three annual harvests in the competition treatment, pooled across all nine environmental blocks. (b) Corresponding distributions shown separately for each environmental block. The bars show the number of pots in which 0–7 individuals with complete aboveground trait measurements were retained, where 7 indicates that all the species in a pot were included in the analysis. Reductions in individual number reflect seedling mortality or missing aboveground traits (e.g. loss of leaves), both of which prevent inclusion in the aboveground multivariate trait space used to estimate ITD. The color shading indicates the number of individuals per pot, and the numbers within the bars denote pot counts.

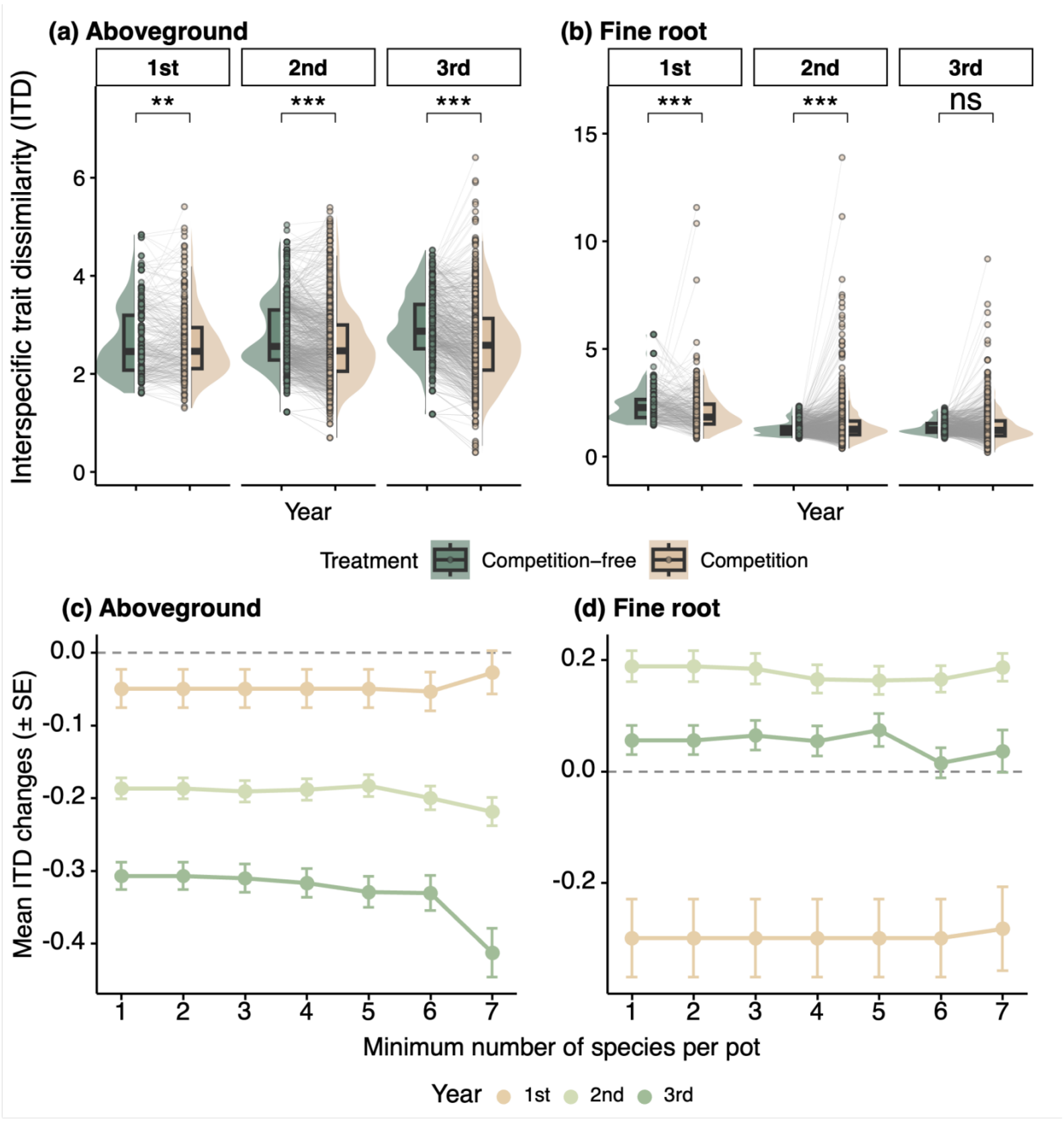

Figure S6 | Pot-level interspecific trait dissimilarity (ITD) and sensitivity to species loss. (a–b) Pot-level ITD for aboveground (a) and fine-root (b) traits across three years. Each point represents the ITD of a focal seedling calculated from its surviving heterospecific neighbors within the same competition pot (2–7 species). To account for variation in species richness due to mortality or missing trait data, each competition pot was paired with a richness-matched expectation generated by resampling individuals from the competition-free treatment (R = 999). Split–violin plots show density distributions with medians and interquartile ranges; grey lines connect observed values to their paired expectations. Asterisks indicate paired test results (**P < 0.01; ***P < 0.001; ns).(c–d) Sensitivity of pot-level changes in ITD to species loss. The mean

change in ITD (±SE) is shown as a function of the minimum number of species retained per pot for the aboveground (c) and fine-root (d) traits. Analyses were restricted to pots meeting each threshold and paired with richness-matched virtual pots from the competition-free treatment.

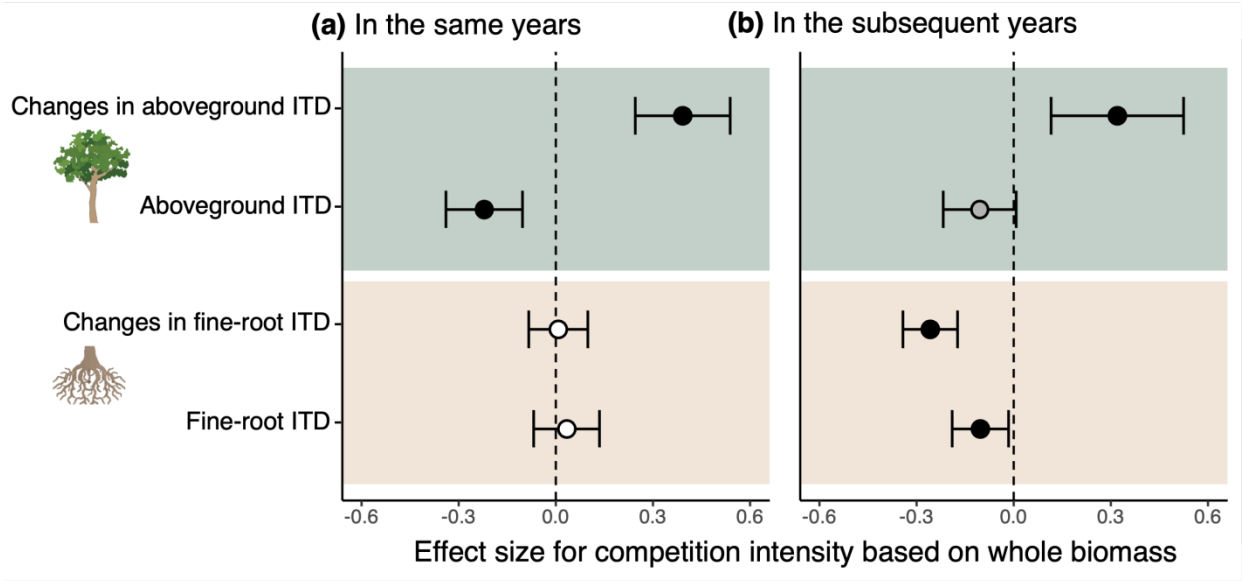

Figure S7 | Pot-level effects of interspecific trait dissimilarity (ITD) on competition intensity. Mixed-effects models relating pot-level ITD metrics to competition intensity (RII) in the same year (a) and the subsequent year (b). ITD was calculated at the pot level between each focal seedling and its surviving neighbors; competition-free expectations were generated using richness-matched, resampled virtual pots. Effect sizes are standardized coefficients from models fitted separately for aboveground and fine-root trait spaces. Solid circles indicate significant effects ($P < 0.05$), open circles indicate nonsignificant effects. Pot-level results are qualitatively consistent with species-level analyses, indicating that the relationship between dynamic ITD shifts and competition intensity is robust to analytical scale.

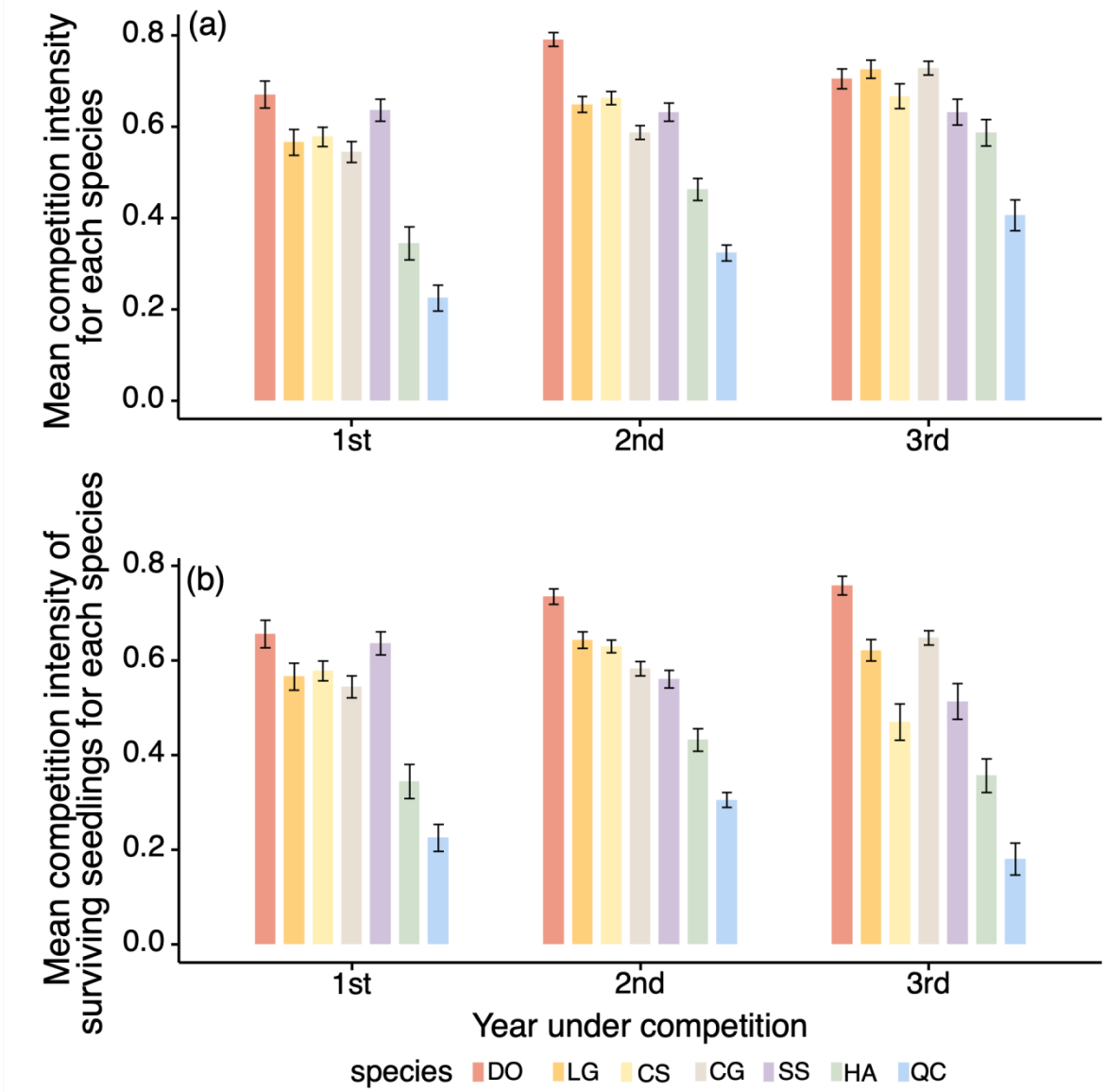

Figure S8 | Species-specific competition intensity across three years in heterogeneous environments. Mean competition intensity (sign-inverted Relative Interaction Index, *RII*; mean ± SE) for seven experimental species measured over the first, second, and third years of competition. Panel (a) shows competition intensity calculated for all individuals of each species, whereas panel (b) shows competition intensity calculated only for surviving seedlings. Competition intensity is based on total biomass, with higher RII values indicating stronger net negative neighbor effects (greater biomass reduction). Different colors represent each species: *Daphniphyllum oldhami* (DO), *Cyclobalanopsis glauca* (CG), *Castanopsis sclerophylla* (CS), *Lithocarpus glaber* (LG), *Schima superba* (SS), *Hovenia acerba* (HA), and *Quercus chenii* (QC). Additional species details are provided in Table S2.

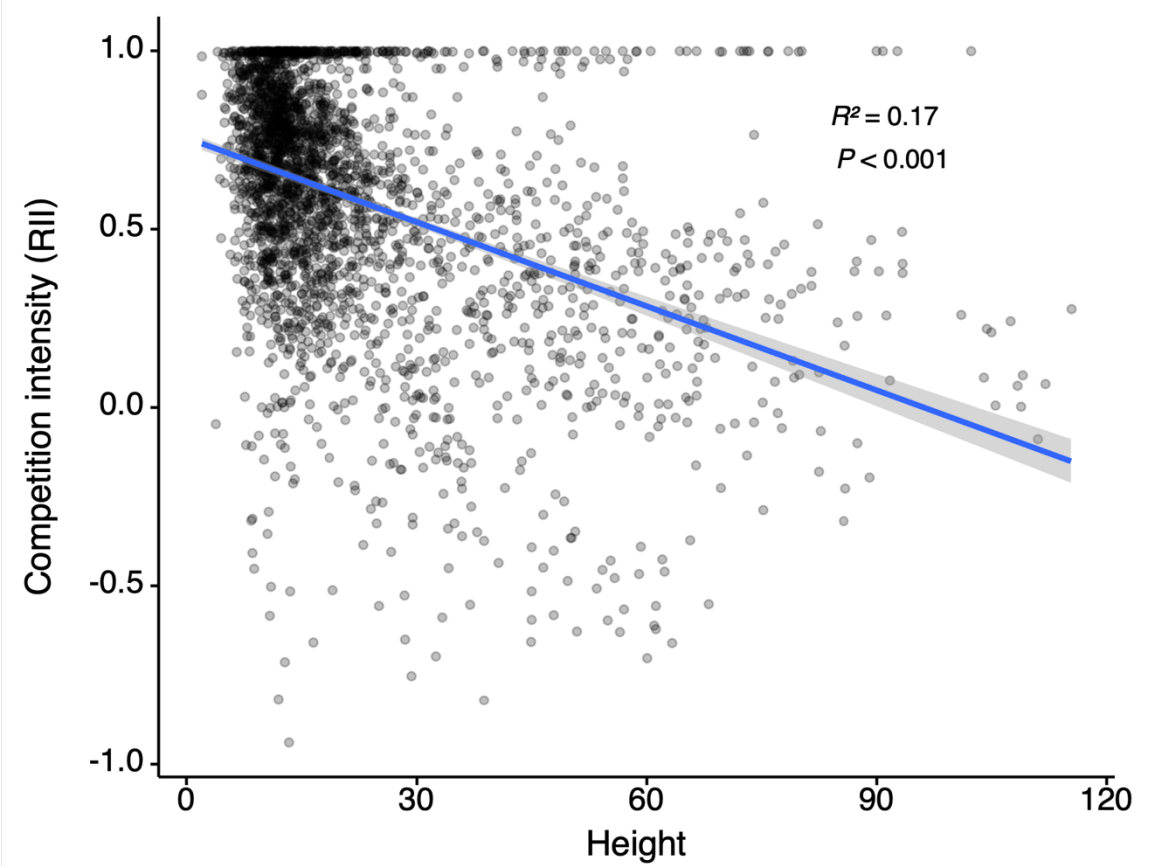

Figure S9 | Relationship between seedling height (cm) and competition intensity. Competition intensity was quantified using the relative interaction intensity (*RII*), calculated as (BM_{alone} - BM_{mixed})/(BM_{alone} + BM_{mixed}), where BM_{mixed} is the biomass of a focal seedling grown with neighbous and BM_{alone} is the mean biomass of conspecific seedlings grown in the competition-free treatment. Points represent individual seedlings, and the solid line shows the fitted linear regression with 95% confidence intervals. Height is measured in centimeters. The weak but significant relationship ($R^2 = 0.17$, $P < 0.001$) indicates that seedling size explains only a modest fraction of variation in competition intensity.

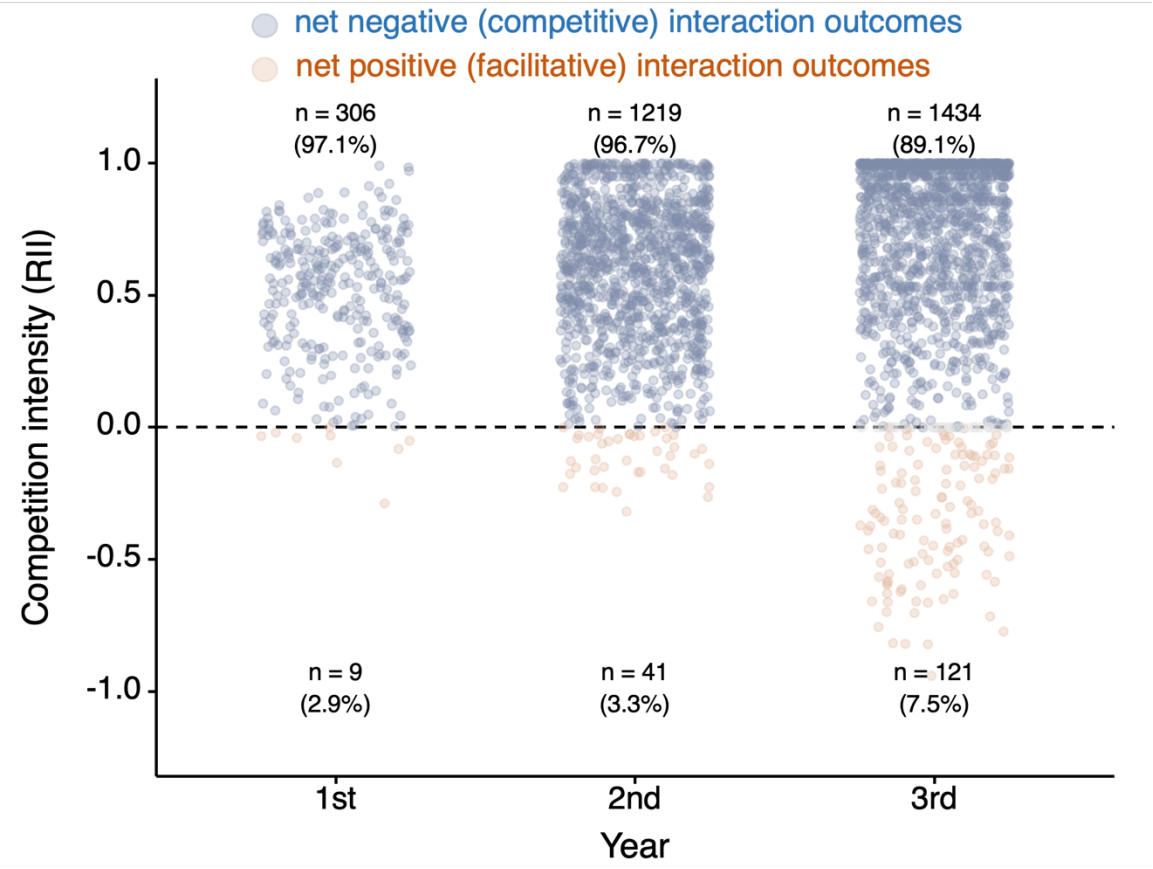

Figure S10 | Year-specific distributions of competition intensity (RII) for seedlings grown with neighbors. Competition intensity was quantified using the relative interaction intensity, which is based on the formulation of Armas et al. (2004) but multiplied by −1 for analytical clarity, and calculated as $(BM_{alone} - BM_{mixed})/(BM_{alone} + BM_{mixed})$ where BM_{mixed} is the biomass of a focal seedling grown with neighbors and BM_{alone} is the mean biomass of conspecific seedlings grown in the competition-free treatment. Under this definition, higher positive values indicate stronger net negative (competitive) interaction outcomes, whereas negative values indicate net positive (facilitative) outcomes. Points represent individual seedlings. The numbers above and below the zero line indicate the count and proportion of seedlings experiencing facilitative and competitive interaction outcomes, respectively.

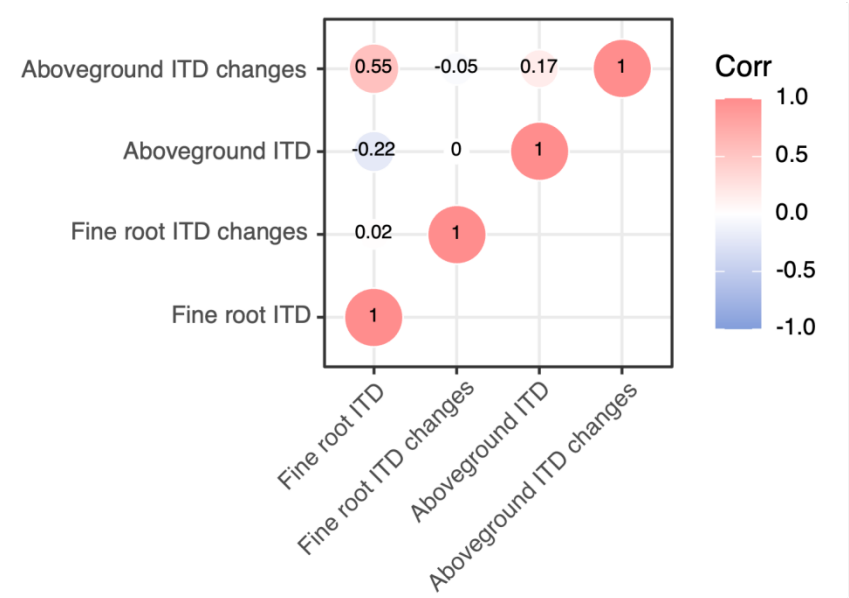

Figure S11 | Pearson correlation matrix showing relationships between interspecific trait dissimilarity (ITD) values and their competition-induced changes across aboveground and fine-root trait spaces. The closer the color is to red, the stronger the positive correlation between the two variables; the closer the color is to blue, the stronger the negative correlation. The numbers represent correlation coefficients, with blank spaces indicating nonsignificant correlations ($P > 0.05$).

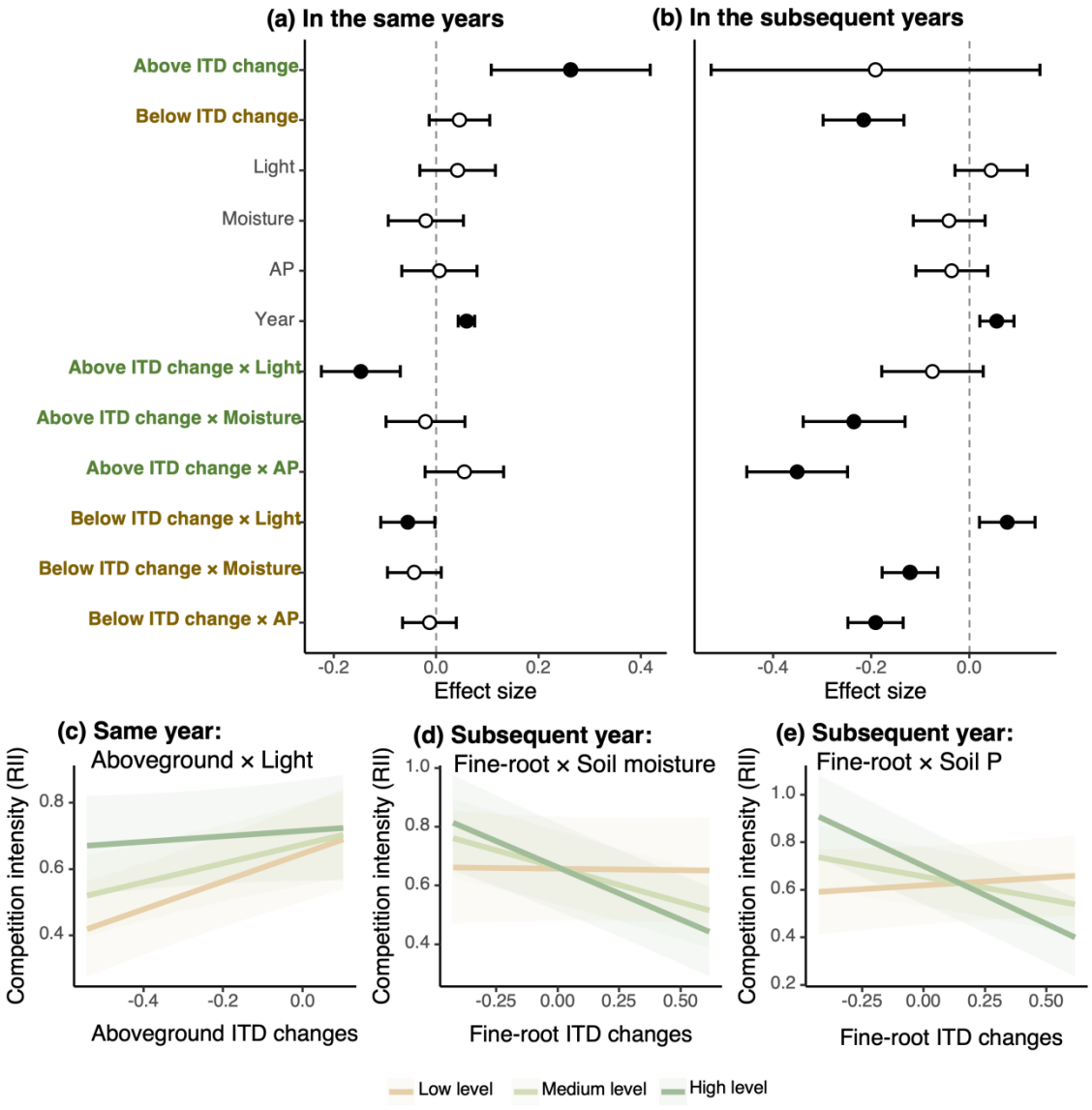

Figure S12 | Context dependence of the relationship between neighbor-induced changes in interspecific trait dissimilarity (ITD) and competition intensity. Panels (a–b) show standardized coefficients (± 95% CI) from mixed-effects models relating competition intensity (sign-inverted RII) to neighbor-induced changes in aboveground and fine-root ITD, environmental conditions (light availability, soil moisture, and available phosphorus), experimental year, and their two-way interactions for the same year (a) and the subsequent year (b). Species identity and environmental block were included as random intercepts. Positive coefficients indicate stronger net competitive effects (higher RII), whereas negative coefficients indicate weaker competition; vertical dashed lines denote zero effects. Panels (c–e) visualize the fitted marginal relationships corresponding to key significant interactions, illustrating how the associations between ITD change and competition intensity varies across environmental contexts. Specifically, panel (c) shows the changes in aboveground ITD under contrasting light availability conditions in the same

year, whereas panels (d) and (e) show the changes in fine-root ITD under contrasting soil moisture and soil phosphorus availability conditions, respectively, in the subsequent year. Lines represent fixed-effect predictions and shaded bands indicate 95% confidence intervals; low, medium, and high environmental levels correspond to representative values observed across experimental blocks.

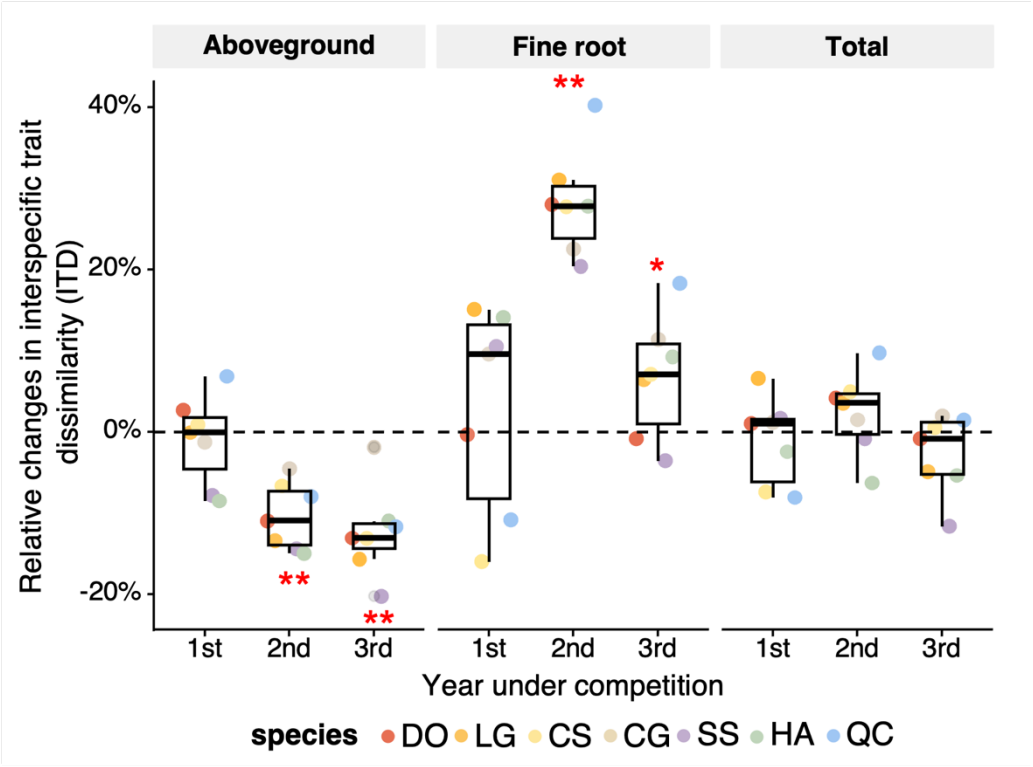

Figure S13 | Relative changes in interspecific trait dissimilarity (ITD) from competition-free to competition conditions in aboveground, fine-root and total trait spaces over the first, second and third years. Interspecific trait dissimilarity (ITD) quantifies the mean Euclidean distance between a focal species and others in multivariate trait space. Relative changes were calculated as the ratio of the absolute ITD change to the baseline ITD under competition-free conditions. The different point colors indicate different species (N = 7). Red asterisks indicate significant ITD changes (paired Wilcoxon rank-sum test; *, P <0.1; *, P <0.05; **, P <0.01; ***, P <0.001).

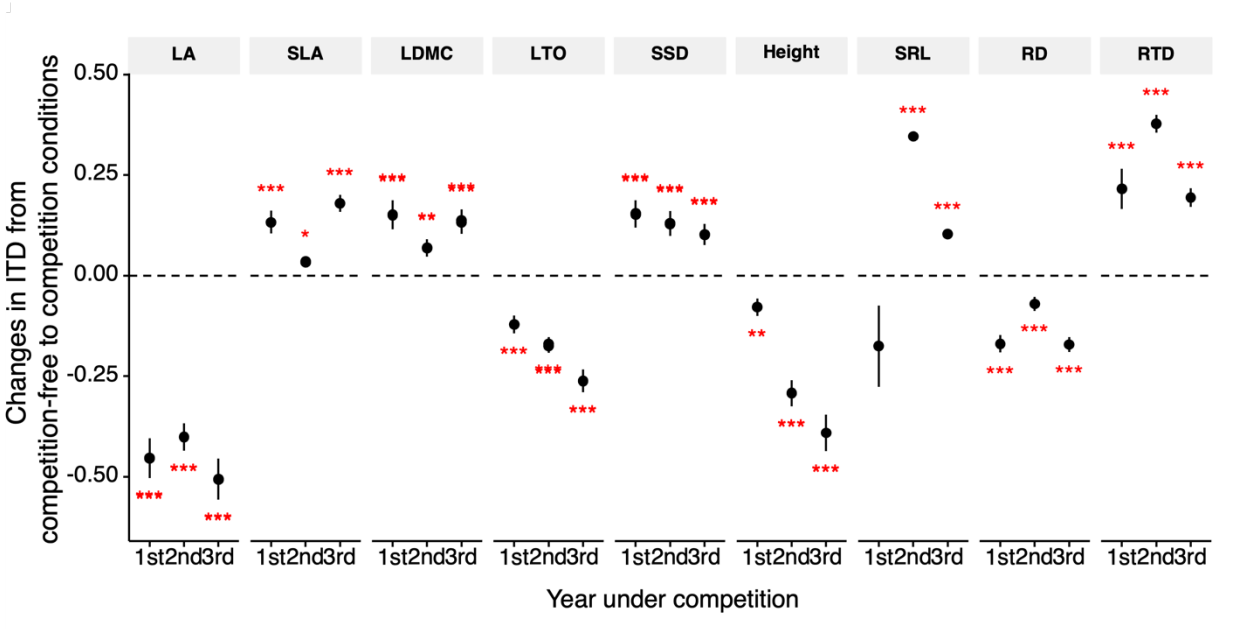

Figure S14 | Changes in interspecific trait dissimilarity (ITD, mean ± SE) from competition-free to competition conditions in individual traits over the first, second and third years. Each black dot represents the mean change (± SE) in ITD between treatments across seven species, calculated as the ITD under competition minus the ITD under competition-free conditions. Red asterisks indicate significant ITD changes (Wilcoxon signed rank test; *, P <0.1; *, P <0.05; **, P <0.01; ***, P <0.001).

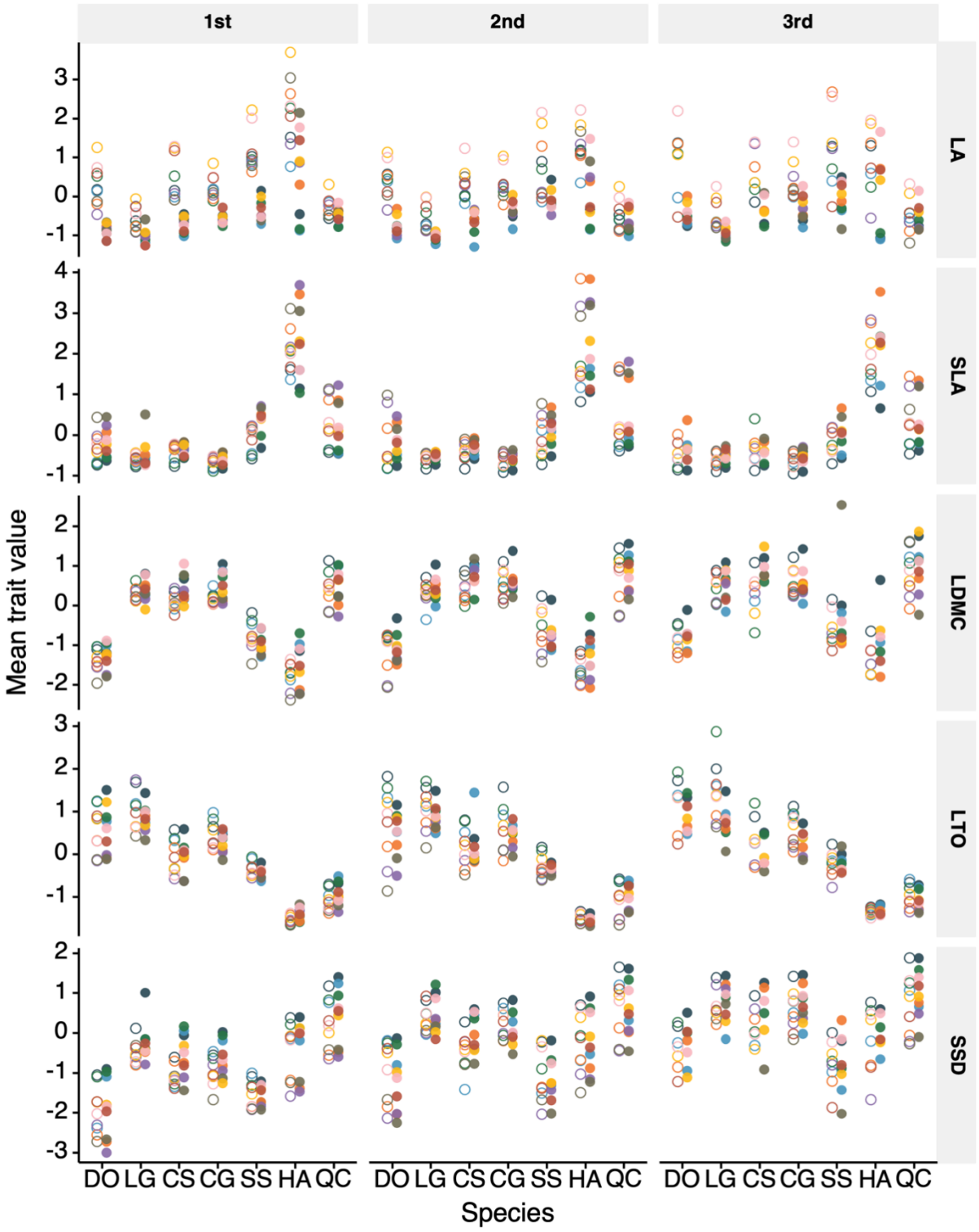
1st
2nd
3rd
LA
SLA
LDMC
LTO
SSD
Mean trait value
DO LG CS CG SS HA QC
Species

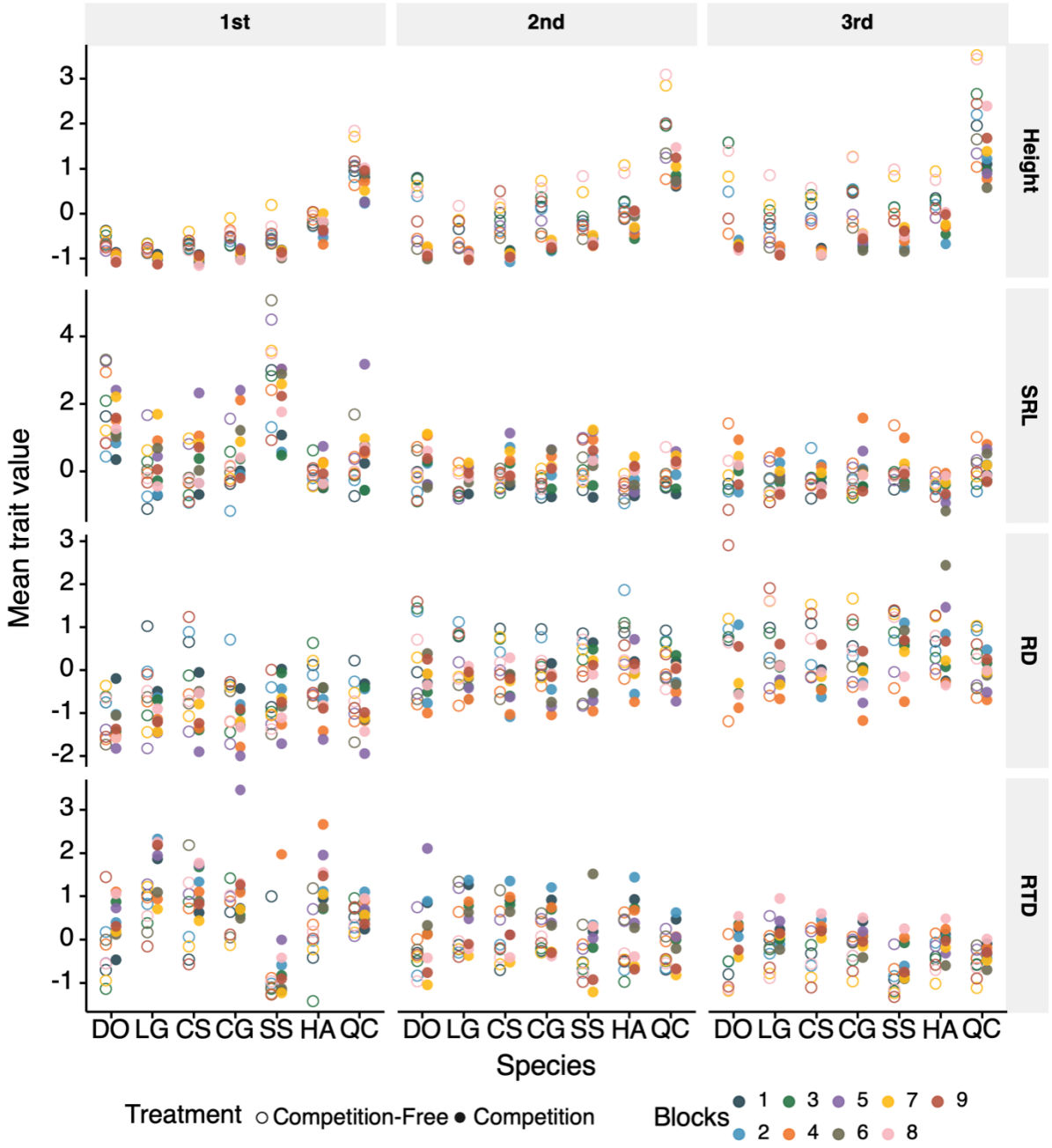

Figure S15 | Mean trait values for seven tree species under competition-free (hollow circles) and competition (solid circles) conditions across nine environmental blocks. Different colors represent environmental blocks, highlighting the variation in average trait values between competition treatments for each species across environments. The species included *Daphniphyllum oldhami* (DO), *Cyclobalanopsis glauca* (CG), *Castanopsis sclerophylla* (CS), *Lithocarpus glaber* (LG), *Schima superba* (SS), *Hovenia acerba* (HA), and *Quercus chenii* (QC).

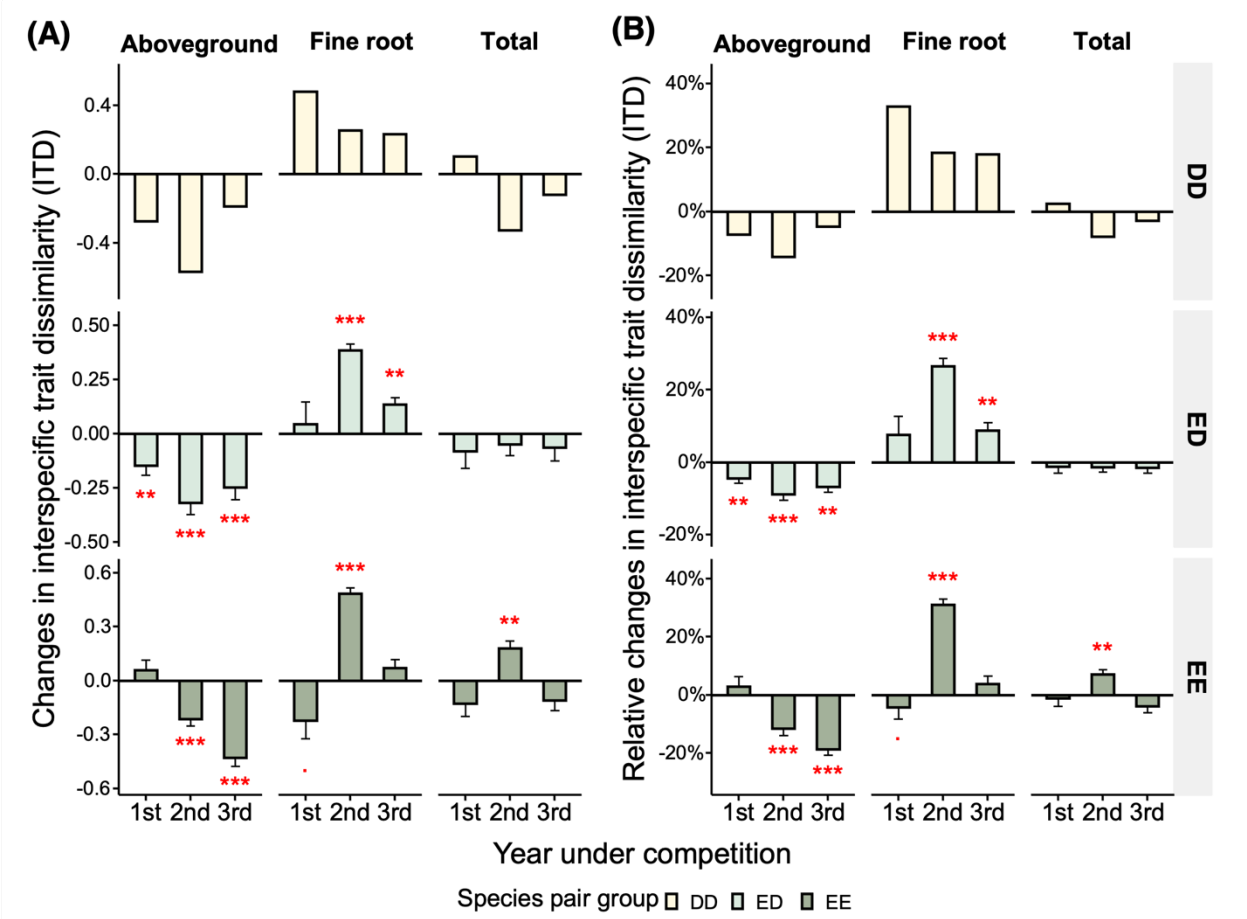

Figure S16 | Competition effects on trait dissimilarity (ITD) across species pairs with different growth forms. (A) Absolute and (B) relative changes in ITD for species pairs grouped by growth form across aboveground, fine-root and total trait spaces over three years. Species combinations include deciduous-deciduous (DD, yellow, n=1 pair), deciduous-evergreen (DE, light green, n=10 pairs), and evergreen-evergreen (EE, dark green, n=10 pairs) combinations. Changes in ITD were calculated as ITD under competition minus ITD under competition-free conditions, with positive values indicating increased trait dissimilarity under competition. Relative changes were calculated by dividing absolute changes by competition-free ITD values. Red asterisks indicate significant ITD changes (Wilcoxon signed rank test, ·: P <0.1; *: P <0.05; **: P <0.01; ***: P <0.001).

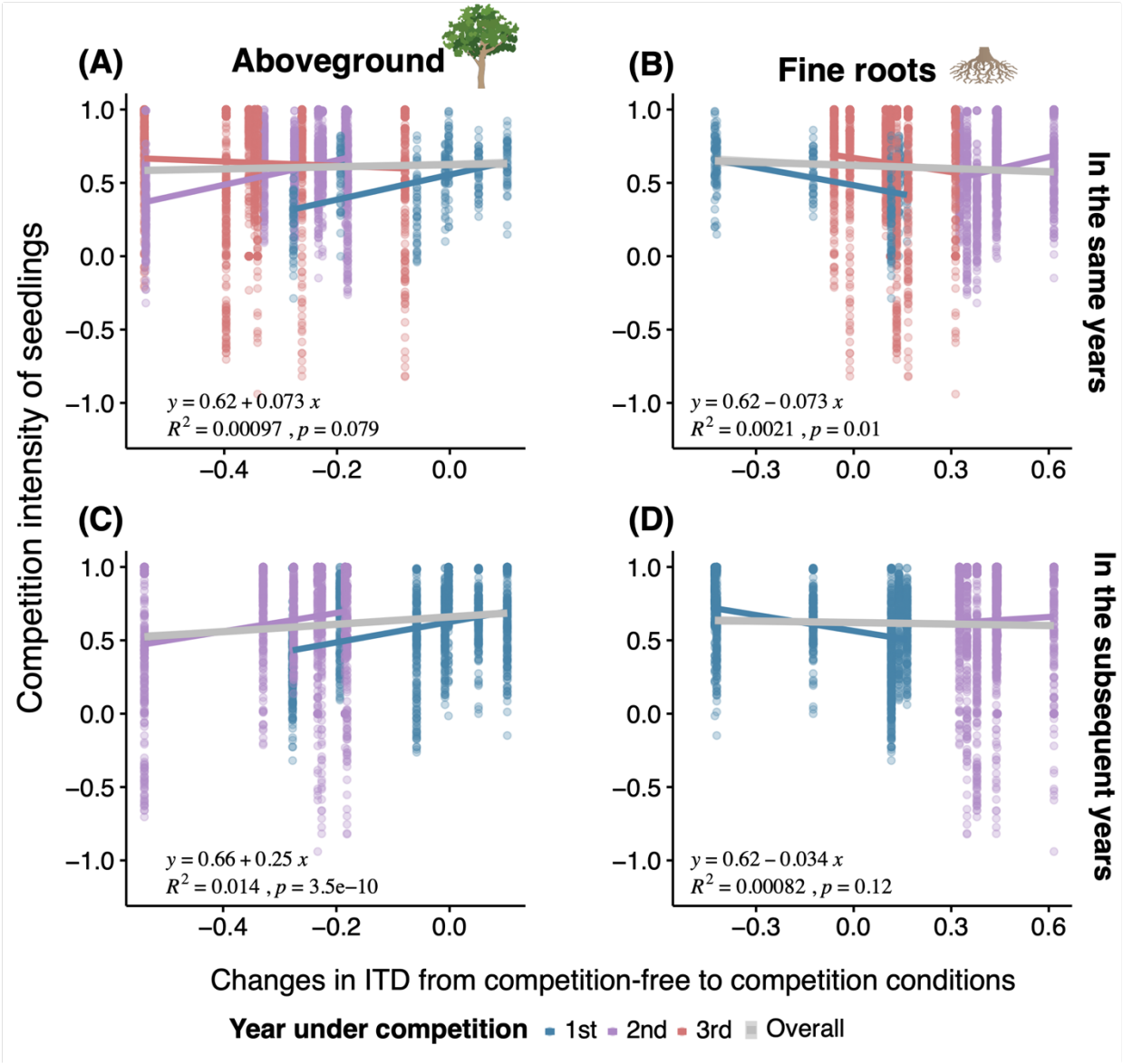

Figure S17 | Relationship between interspecific trait dissimilarity (ITD) changes and competition intensity in the current year (A, B) and subsequent years (C, D) for aboveground (A, C) and fine-root (B, D) trait spaces. Each point represents an individual seedling, with colors indicating first (blue), second (purple), and third (red) years of competition. Changes in ITD were calculated as the ITD under competition minus the ITD under competition-free conditions. The competition intensity was measured via the inverse relative interaction index (*RII*) based on total biomass, with higher values indicating greater biomass reduction. The gray lines represent simple linear regression relationships across all years, with equations and significance values displayed.

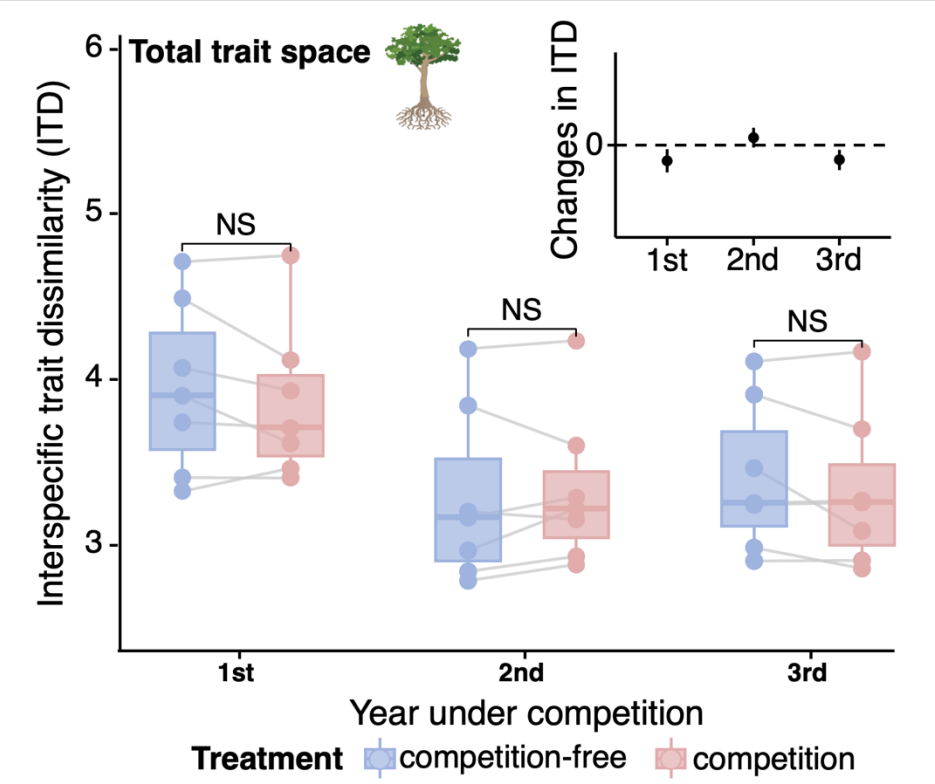

Figure S18 | Competition effects on interspecific trait dissimilarity (ITD) in total trait space across three years. ITD in total trait space under competition-free (blue) and competition (pink) treatments across three years. ITD quantifies the mean Euclidean distance between a focal species and others in a four-dimensional trait space derived from principal component analysis of nine functional traits, with larger values indicating greater trait dissimilarity. The colored points represent species-specific ITD values ($N = 7$), with gray lines connecting the same species across treatments. The top-right inset shows the mean changes (± SEs) in the ITD between treatments, calculated as the ITD under competition minus the ITD under competition-free conditions. Positive values indicate greater dissimilarity under competition, whereas negative values suggest trait convergence under competitive pressure. NS indicates nonsignificant changes between treatments (Wilcoxon signed-rank test).

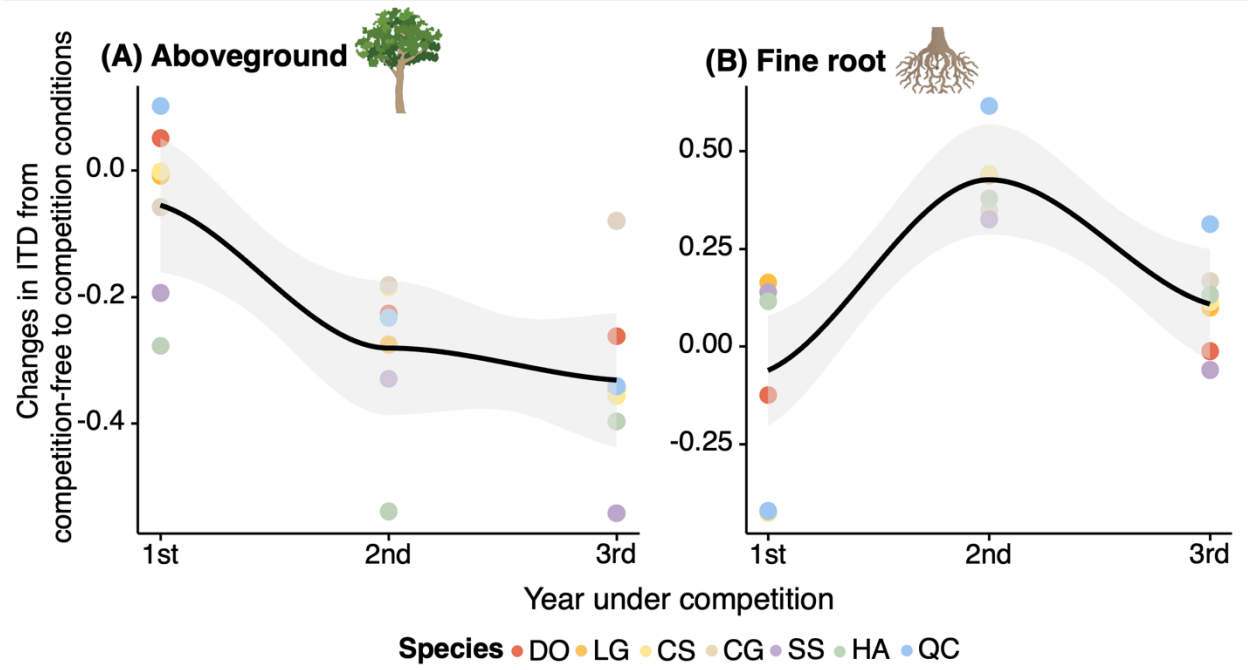

Figure S19 | Temporal dynamics of competition-induced interspecific trait dissimilarity (ITD) changes across species. Mean changes in ITD for aboveground (A) and fine-root (B) trait spaces across three years of competition. ITD represents the mean Euclidean distance between focal species and competitors in multivariate trait space. Changes in ITD were calculated as ITD under competition minus ITD under competition-free conditions for each species, with negative values indicating reduced trait dissimilarity under competition. The black curves show locally weighted smoothing (loess regression) with 95% confidence intervals (gray shading). The colored points represent individual species: *Daphniphyllum oldhami* (DO), *Cyclobalanopsis glauca* (CG), *Castanopsis sclerophylla* (CS), *Lithocarpus glaber* (LG), *Schima superba* (SS), *Hovenia acerba* (HA), and *Quercus chenii* (QC).

References

Bennett, J. A., Riibak, K., Tamme, R., Lewis, R. J., & Pärtel, M. (2016). The reciprocal relationship between competition and intraspecific trait variation. *Journal of Ecology*, *104*(5), 1410–1420. https://doi.org/10.1111/1365-2745.12614

Carmona, C. P., de Bello, F., Azcárate, F. M., Mason, N. W. H., & Peco, B. (2019). Trait hierarchies and intraspecific variability drive competitive interactions in Mediterranean annual plants. *Journal of Ecology*, *107*(5), 2078–2089. https://doi.org/10.1111/1365-2745.13248

Fort, F., Cruz, P., & Jouany, C. (2014). Hierarchy of root functional trait values and plasticity drive early-stage competition for water and phosphorus among grasses. *Functional Ecology*, *28*(4), 1030–1040. https://doi.org/10.1111/1365-2435.12217

He, Y., Liu, H., Yang, Q., Cao, Y., Yin, H., Zhou, Z., Yu, Q., & Wang, X. (2022). Neighborhood effects on tree mortality depend on life stage of neighbors. *Frontiers in Plant Science*, *13*(838046). https://doi.org/10.3389/fpls.2022.838046

Kraft, N. J. B., Crutsinger, G. M., Forrestel, E. J., & Emery, N. C. (2014). Functional trait differences and the outcome of community assembly: An experimental test with vernal pool annual plants. *Oikos*, *123*(11), 1391–1399. https://doi.org/10.1111/oik.01311

Kraft, N. J. B., Godoy, O., & Levine, J. M. (2015). Plant functional traits and the multidimensional nature of species coexistence. *Proceedings of the National Academy of Sciences*, *112*(3), 797–802. https://doi.org/10.1073/pnas.1413650112

Kunstler, G., Falster, D., Coomes, D. A., Hui, F., Kooyman, R. M., Laughlin, D. C., Poorter, L., Vanderwel, M., Vieilledent, G., Wright, S. J., Aiba, M., Baraloto, C., Caspersen, J., Cornelissen, J. H. C., Gourlet-Fleury, S., Hanewinkel, M., Herault, B., Kattge, J., Kurokawa, H., … Westoby, M. (2016). Plant functional traits have globally consistent effects on competition. *Nature*, *529*(7585), Article 7585. https://doi.org/10.1038/nature16476

Kunstler, G., Lavergne, S., Courbaud, B., Thuiller, W., Vieilledent, G., Zimmermann, N. E., Kattge, J., & Coomes, D. A. (2012). Competitive interactions between forest trees are driven by species' trait hierarchy, not phylogenetic or functional similarity: Implications for forest community assembly. *Ecology Letters*, *15*(8), 831–840. https://doi.org/10.1111/j.1461-0248.2012.01803.x

Lyu, S., & Alexander, J. M. (2024). Functional traits predict outcomes of current and novel competition under warmer climate. *Global Change Biology*, *30*(11), e17551. https://doi.org/10.1111/gcb.17551

Lyu, S., Liu, X., Venail, P., & Zhou, S. (2017). Functional dissimilarity, not phylogenetic relatedness, determines interspecific interactions among plants in the Tibetan alpine meadows. *Oikos*, *126*(3), 381–388. https://doi.org/10.1111/oik.03378

Mahaut, L., Violle, C., Shihan, A., Pélissier, R., Morel, J.-B., de Tombeur, F., Rahajaharilaza, K., Fabre, D., Luquet, D., Hartley, S., Thorne, S. J., Ballini, E., & Fort, F. (2023). Beyond trait distances: Functional distinctiveness captures the outcome of plant competition. *Functional Ecology*, *37*(9), 2399–2412. https://doi.org/10.1111/1365-2435.14397

Pérez-Ramos, I. M., Matías, L., Gómez-Aparicio, L., & Godoy, Ó. (2019). Functional traits and phenotypic plasticity modulate species coexistence across contrasting climatic conditions. *Nature Communications*, *10*(1), Article 1. https://doi.org/10.1038/s41467-019-10453-0

Qi, J., Xie, D., Yin, T., Yan, G., Gastellu-Etchegorry, J.-P., Li, L., Zhang, W., Mu, X., & Norford, L. K. (2019). LESS: LargE-Scale remote sensing data and image simulation framework over heterogeneous 3D scenes. *Remote Sensing of Environment*, *221*, 695–706. https://doi.org/10.1016/j.rse.2018.11.036

Wagg, C., Ebeling, A., Roscher, C., Ravenek, J., Bachmann, D., Eisenhauer, N., Mommer, L., Buchmann, N., Hillebrand, H., Schmid, B., & Weisser, W. W. (2017). Functional trait dissimilarity drives both species complementarity and competitive disparity. *Functional Ecology*, *31*(12), 2320–2329. https://doi.org/10.1111/1365-2435.12945

Yang, J., Wang, X., Carmona, C. P., Wang, X., & Shen, G. (2024). Inverse relationship between species competitiveness and intraspecific trait variability may enable species coexistence in experimental seedling communities. *Nature Communications*, *15*(1), 2895. https://doi.org/10.1038/s41467-024-47295-4

Yin, D., Liu, Y., Ye, Q., Cadotte, M. W., & He, F. (2021). Trait hierarchies are stronger than trait dissimilarities in structuring spatial co-occurrence patterns of common tree species in a subtropical forest. *Ecology and Evolution*, *11*(12), 7366–7377. https://doi.org/10.1002/ece3.7567

Yu, Q., Yang, J., & Shen, G. (2022). Relationship between canopy structure and species composition of an evergreen broadleaf forest in Tiantong region, Zhejiang, China. *Chinese Journal of Plant Ecology*, *46*(5), 529. https://doi.org/10.17521/cjpe.2022.0047